Inhomogeneous shear flows of wormlike micelles: A master dynamic phase diagram

Jean-François Berret and Grégoire Porte
Groupe de Dynamique des Phases Condensées, Unité Mixte de Recherches CNRS/Université de Montpellier II No. 5581, Université de Montpellier II, F-34095 Montpellier Cedex 05, France

Jean-Paul Decruppe
Laboratoire de Physique des Liquides et Interfaces, Groupe de Physique des Colloides et Polymères, Université de Metz, 57078 Metz, France

(Received 29 July 1996)

We report on the nonlinear mechanical response of surfactant wormlike micelles subjected to steady shear flow. The system placed under scrutiny is made of cetylpyridinium chloride, sodium salicylate, and salted water at 0.5*M* NaCl (abbreviated as CPCl-Sal). We have investigated solutions in the intermediate concentration ranges, at $\phi=6\%$, 8% and $\phi=12\%$ for temperatures ranging between 20 °C and 50 °C. In these T and ϕ ranges, we first confirm that the present system is a true Maxwell fluid. As a consequence, the nonlinear rheology can be formulated in terms of the normalized quantities, $\sigma^*=\sigma/G_0$ and $\dot{\gamma}^*=\dot{\gamma}\tau_R$, where G_0 is the elastic plateau modulus and τ_R the terminal relaxation time of the Maxwell fluid. Second, we demonstrate that the flow curves of the CPCl-Sal wormlike micelles σ^* ($\dot{\gamma}^*$) are invariant with respect to relative changes in temperature and concentration. This enables us to define superimposition procedures between flow curves obtained at different temperatures and concentrations and to derive the so-called ''master dynamic phase diagram'' of the CPCl-Sal wormlike micelles. One crucial feature of this master phase diagram is the existence of a critical behavior at $T=T_c$. Here, the stress σ^* levels off progressively up to a plateau that is reduced to a single flat point of coordinates ($\sigma^*=0.9$, $\dot{\gamma}^*=3$). The low-temperature regime ($T<T_c$) is again identified by a shear stress plateau beginning by a true discontinuity of slope in the σ^* ($\dot{\gamma}^*$) behavior. At high T ($>T_c$), σ^* increases monotonously at all shear rates. In order to examine the state of shearing at the stress plateau, flow birefringence experiments were undertaken with a rheo-optical device working with polarized light propagating parallel to the vorticity axis of the Couette. In the plateau regime, the flow is clearly inhomogeneous. Within the gap of a cell, two phases of very different birefringence are observed in the steady state of shearing, as well as after cessation of the shearing. [S1063-651X(97)07701-5]

PACS number(s): 82.70.−y, 83.50.Gd, 47.20.Ft, 47.50.+d

I. INTRODUCTION

The shear flow properties of solutions of wormlike micelles have been subjected to an intense debate during the past few years. Wormlike micelles are long flexible aggregates made of common surfactant molecules, and in solution in water, they are producing highly viscoelastic fluids [1]. Besides industrial purposes, one reason for this interest is certainly related to the good theoretical understanding of the dynamics of the wormlike micelles when subjected to a weak mechanical deformation (linear viscoelasticity). As far as the linear rheology is concerned, there is an excellent overall agreement between theoretical predictions and experimental measurements: the linear viscoelasticity at low frequencies ($\omega<100$ rad s^{-1}) has been found to be that of a Maxwell fluid [2]. In other words, in the corresponding time range ($t>10$ ms) the stress relaxation function $G(t)$ is decreasing monoexponentially and reads $G(t)=G_0\exp(-t/\tau_R)$ where G_0 is the elastic plateau modulus and τ_R the terminal relaxation time. G_0 is associated with the degree of entanglement of the network in the semidilute regime and τ_R takes into account the two fundamental motional dynamics of the wormlike micellar chains: reptation and reversible breaking. These later aspects have been treated in detail in Refs. [2–4].

There is another experimental situation for which a general agreement has emerged from recent literature. It concerns the concentrated solutions of wormlike micelles at the vicinity of the isotropic-to-nematic (I-N) phase boundary. Several surfactant systems investigated these last three years exhibit a nematic phase of micelles at concentrations as high as $\phi_{I\text{-}N}\sim30\%$ [5–8]. This nematic state is understood as resulting from the steric interactions between micellar threads. When an isotropic solution with ϕ slightly below $\phi_{I\text{-}N}$ is subjected to a simple shearing flow, a shear-induced transition from an isotropic to a nematic state has been evidenced [5,6]. One of the first experimental evidences of the shear-induced I-N transition was due to neutron scattering under shear for solutions of $CPClO_3$-$NaClO_3$ [5] and of CPCl-hexanol-brine [6]. Above a characteristic shear rate $\dot{\gamma}_{I\text{-}N}$, the small-angle neutron patterns become anisotropic and finally reveal the coexistence of two phases of different scattering signatures: the isotropic and the nematic phases. This picture was later on confirmed by flow birefringence on cetyltrimethylammonium bromide (CTAB) solutions close to the nematic state [8,9]. Looking at the gap in the direction of the vorticity of a light transparent Couette cell, the existence of the two-phase state under shear (isotropic-nematic) was also directly visualized above $\dot{\gamma}_{I\text{-}N}$ [8,9].

As far as the mechanical response to constant shear rates is concerned, a general behavior of the shear stress σ versus shear rate has been found to be shared in common by all

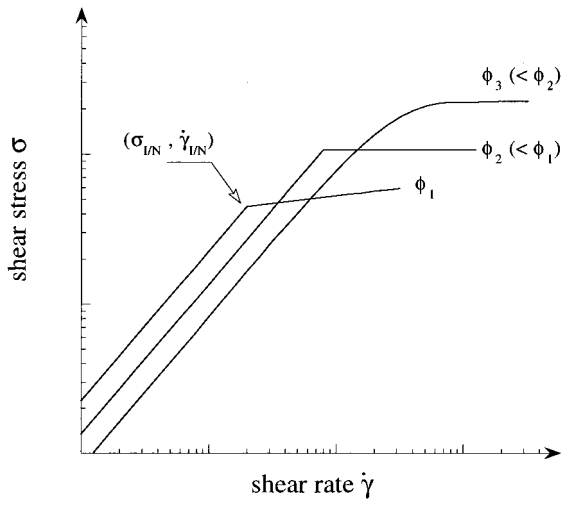

FIG. 1. Schematical flow curves for wormlike micelles as obtained from mechanical rate controlled experiments. The curves labeled 1, 2, and 3 are for decreasing surfactant concentrations, $\phi_1 > \phi_2 > \phi_3$, ϕ_1 being the closest to the concentration of isotropic-to-nematic transition (in absence of shear). For this latter concentration, one defines $(\sigma_{I\text{-}N}, \dot{\gamma}_{I\text{-}N})$ as the coordinates of the crossover between the Newtonian and the power-law regime.

these concentrated surfactant systems. In a controlled shear rate experiment, as $\dot{\gamma}$ is increased, the stress increases linearly (in the Newtonian regime) and then very abruptly at $\dot{\gamma}_{I\text{-}N}$ a crossover occurs to a power-law regime $\sigma \sim \dot{\gamma}^a$. Exponents a were found to range between 0.1 and 0.2 in $CPClO_3$ [5], CPCl-hexanol [6,10], CPCl-Sal [7], and CTAB [11] solutions. A schematic representation of the flow curve is provided in Fig. 1 for concentrated solutions of wormlike micelles (curve labeled $\phi_1 < \phi_{I\text{-}N}$). A crucial feature of the *I-N* transition at high concentrations is that the crossover defined at $\dot{\gamma}_{I\text{-}N}$ and $\sigma_{I\text{-}N}$ (see Fig. 1) occurs *well inside* the Newtonian regime. In other words, the relation

$$\sigma_{\mathrm{I\text{-}N}} \approx \eta_0 \dot{\gamma}_{\mathrm{I\text{-}N}} \tag{1}$$

stands where η_0 is the static viscosity. Assuming $\eta_0 = G_0 \tau_R$ for a Maxwellian fluid and taking for G_0 the elastic plateau modulus usual values of about 500 Pa [7], Eq. (1) is equivalent to

$$\frac{\sigma_{I\text{-}N}}{G_0} \approx \dot{\gamma}_{I\text{-}N} \tau_R \ll 1. \tag{2}$$

Equation (2) already points out the relevance of using reduced or normalized units for these wormlike systems. This will be systematically extended in the following. It also emphasizes that the reduced stress and rate of transition are equal and much lower than one (by over a decade). Physically, Eqs. (1) and (2) mean that modest shearing fields are sufficient to trigger the transition for concentrated solutions. On the theoretical side, a complete treatment of the first-order *I-N* transition induced by simple shear is still missing for the wormlike micelles [12].

Upon decreasing concentration, the steady shear properties of wormlike micelles are much less understood, even on the experimental side. Salient features are, however, observed experimentally on several systems, which Fig. 1 aims to illustrate. As ϕ is decreased, the static viscosity η_0 decreases, as a result of the lowering of the elastic modulus G_0. The above change in the stress evolution experienced for $\phi \sim \phi_{I\text{-}N}$ at $(\sigma_{I\text{-}N}, \dot{\gamma}_{I\text{-}N})$ is now shifted to higher shear rates, and the stress exhibits a true plateau in the second part of the flow curve (curve labeled 2 in Fig. 1). At still higher dilution (labeled 3), the transition toward the plateau regime is much softer and the stress levels off with no clear discontinuity of slope. This progressive change of the nonlinear response of wormlike micelles upon dilution was first recognized in the two systems already mentioned, namely, in $CPClO_3$-$NaClO_3$ [5] and in CPCl-Sal [7]. In the meantime, similar behaviors were found out in CPCl-hexanol-brine [6] and in CTAB [8] solutions, especially in relation to behaviors 1 and 2 of Fig. 1. The CPCl-Sal system deserves an additional comment: In contradistinction with the three other surfactants mentioned previously, the basic behaviors of Fig. 1 extend to concentrations as low as $\phi \sim 6\%$, a concentration which is believed to be the upper limit of the semidilute regime [13]. A full understanding of the sequence recognized in Fig. 1 with decreasing ϕ is, unfortunately, missing. However, shear stress plateaus are rheological features that were also encountered experimentally in semidilute wormlike micellar solutions [1], i.e., $\phi \sim 1\%$. Note that these concentrations are less or much less than those discussed in the schematical Fig. 1. For this specific ϕ regime, the plateau behavior was theoretically interpreted in terms of a pure mechanical instability of shear-banding type [14,15].

In the present paper, we extend our preceding experimental study on the CPCl-Sal wormlike micelles [7], hereafter referred to as I, and provide now strong experimental indications of the relationship between the plateau regime and the existence of inhomogeneous flow of the solution. Using empirically determined superimposition procedures, we could sum up the flow behaviors at many different concentrations and temperatures on one single master ''dynamic phase diagram.'' This phase diagram follows the general evolution described in Fig. 1 above, and this generality arises from the fact that it uses the reduced rheological quantities σ/G_0 and $\dot{\gamma}\tau_R$ instead of σ and $\dot{\gamma}$. We show the existence of critical flow conditions given by $\sigma/G_0 = 0.9$ and $\dot{\gamma}\tau_R \sim 3$, which are invariant upon concentration or temperature changes. In the present paper, the high concentration range referring to curve 1 in Fig. 1 will not be addressed. New results using flow birefringence experiments are provided at last to demonstrate that in the plateau regime, the wormlike micelles flow inhomogeneously. Within the gap of a Couette cell, two phases of very different birefringence are observed in the steady state of shearing, as well as after cessation of the shearing.

The paper is organized as follows: After a brief description of the experimental procedure (Sec. II), The Maxwellian character of the CPCl-Sal micelles is emphasized (Sec. III). Section IV is dedicated to the rheological nonlinear responses as functions of temperature and concentration and to the determination of superposition procedures applied to different flow curves expressed in normalized units, σ/G_0 and $\dot{\gamma}\tau_R$. The master ''dynamic phase diagram'' is then derived using a ''reduced temperature'' as the control parameter. In

Sec. VI the present set of data is compared to our previous works on CPCl-Sal wormlike micelles and discussed in light of some theoretical predictions on the isotropic-nematic transition predicted for low molecular weight thermotropic liquid crystal [16,17]. We show, before some concluding remarks, photographs of a sheared sample in the plateau regime, exhibiting clearly the coexistence under shear of two different phases, characterized by very different birefringence.

II. EXPERIMENT

The surfactant solutions investigated here are the binary mixtures made of cetylpyridinium chloride (CP^+,Cl^-) and sodium salicylate (Na^+,Sal^-) (hereafter abbreviated as CPCl-Sal) diluted in 0.5*M* NaCl-brine. Extensively studied by Hoffmann and Rehage [1,18] but essentially without added salt, this system is known to easily form elongated wormlike micelles. Following our two first reports on the CPCl-Sal system, we focus here on the intermediate concentration range, between semidilute (ϕ=0.5–5 % [13]) and concentrated (ϕ>20%) solutions. The weight percent concentrations selected for the present study were ϕ=6%, 8%, and 12% with a molar ratio R=[Sal]/[CPCl]=0.5.

The phase diagram of CPCl-Sal solutions has been discussed in detail in I. Derived using x-ray and birefringence measurements at T=30 °C, the (ϕ_{CPCl},ϕ_{Sal})-phase diagram exhibits the usual sequence of phases, namely, isotropic (L_1), nematic, and hexagonal with increasing ϕ. The nematic calamitic (N_c) region is observed for total surfactant concentration $\phi=\phi_{CPCl}+\phi_{Sal}\sim$36%. This is to emphasize that the solutions placed under scrutiny here are far from the isotropic-nematic phase boundary.

The linear and nonlinear viscoelastic properties of the CPCl-Sal solutions were obtained on a rheometrics fluid spectrometer (RFS II) working in a cone-and-plate configuration with controlled shear rate (diameter 50 and 30 mm, angle 0.02 rad). Dynamical measurements were carried out for angular frequency ω=0.1–100 rad s^{-1} at temperatures ranging between T=20 °C and T=50 °C. It should be pointed out that this narrow T interval was dictated by the physicochemical properties of the surfactant solutions: The Kraft temperature is about 19 °C. In addition, for a system with a relaxation time of the order of 1 s at room temperature, τ_R falls out of the frequency limits of the fluid spectrometer utilized, namely, τ_R<10 ms above 50 °C.

Steady shear rate measurements were restricted to $\dot{\gamma}$ not larger than some hundred of s^{-1}, because of mechanical flow instabilities such as elastically driven meniscus distortions [19]. It should be pointed out first that all the data displayed in the following have been obtained using controlled-rate rheometer. In other words, the solution was forced to flow at a macroscopic imposed shear rate $\dot{\gamma}$, yielding a shear stress $\sigma(\dot{\gamma})$. Second, we are here essentially concerned with the stationary limit of the stress. It is now well established—as shown in I—that long-lasting transient responses $\sigma(t)$ are typical features of the nonlinear rheology of wormlike micelles in the plateau region (see Fig. 1), and so we consider here the long-time limit only (stationary state of shearing). Third, we have also checked that the flow curves are reproducible using either a Couette cell with controlled rate or using a cone-and-plate device at imposed stress [20].

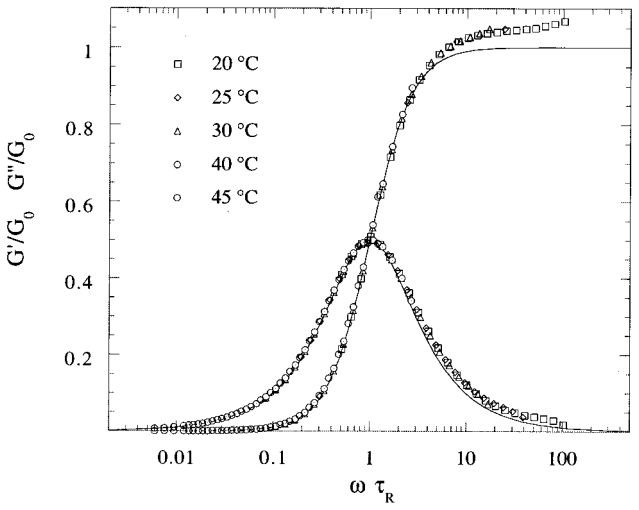

FIG. 2. CPCl-Sal-H_2O (0.5*M* NaCl), ϕ=12%: Real and imaginary parts of the complex elastic modulus $G^*(\omega)=G'(\omega)+iG''(\omega)$ in units of G_0 as functions of the rescaled angular frequency $\omega\tau_R$ for temperatures comprised between 20 °C and 45 °C. The solid lines are explained in the text and correspond to the Maxwellian viscoelastic behavior.

III. LINEAR REGIME: PURE MAXWELL BEHAVIOR

A detailed account of the linear rheology of CPCl-Sal wormlike micelles at ambient temperature has been already provided in our earlier reports [7,13]. As a result, it was found that solutions in the intermediate regime of concentration behave as almost exact Maxwell fluids. The low-frequency linear response is thus entirely described by two parameters, the elastic plateau modulus G_0 and the terminal relaxation time τ_R. We here undertook dynamical measurements at temperatures varying from 20 °C to 50 °C for the three samples considered (ϕ=6%, 8%, and 12%). Figure 2 shows the results of these dynamical frequency sweeps in rescaled units. The storage modulus $G'(\omega)$ and the loss modulus $G''(\omega)$ as received from the 12% solutions were divided by G_0 and plotted against the reduced frequency $\omega\tau_R$. The agreement with a Maxwell model is excellent at all temperatures and only slight deviations are observed at $\omega\tau_R$>10. The continuous lines of Fig. 2 are $G'(x)/G_0=x^2/(1+x^2)$ and $G''(x)/G_0=x/(1+x^2)$ where $x=\omega\tau_R$. Figure 2 enables us to conclude that in the T range investigated the CPCI-Sal solutions still behave as Maxwell fluids.

Temperature evolutions for G_0 and τ_R can thus be derived for the three samples investigated according to a simple Maxwell analysis. The plateau modulus is found to vary as $G_0\sim T$ between 20 and 50 °C, whereas in the same range τ_R obeys an Arrhenius law, $\tau_R\sim\exp(E_A/T)$. E_A denotes here some activation energy taking into account the reversible scission mechanism of the micelles as well as the endcap energy [2,21]. Values for G_0 and τ_R as received from the 20 °C data are listed in Table I for comparison. Also shown are the energy barriers E_A and the slope of the linear variation of the elastic plateau modulus G_0/T. Note for this last ratio that a temperature variation by 30 K only changes the G_0 data by 10%, which is only twice the experimental accu-

TABLE I. List of the room-temperature ($T=25$ °C) viscoelastic constants measured for the three CPCl-Sal concentrations investigated here. G_0 denotes the elastic plateau modulus and τ_R the terminal relaxation time. The activation energy E_A (expressed in units of k_BT, $T=300$ K) was deduced from the temperature dependence of the Maxwell time.

ϕ (%)	G_0 (Pa)	G_0/T (Pa/K)	τ_R (ms)	E_A (K)
6	62	0.22	990	53.8±0.2
8	106	0.37	1070	55.9±0.2
12	235	0.8	1020	54.9±0.3

racy in determining G_0. The precision on the data of the third column in Table I should not be overestimated.

IV. NONLINEAR REGIME: SHEAR-TEMPERATURE-CONCENTRATION SUPERPOSITIONS

The careful determination of the Maxwell parameters as functions of temperature is motivated in the following by the search of a universal representation of the flow curves in terms of σ/G_0 versus $\dot{\gamma}\tau_R$. It is worthwhile to remember that measurements have been performed under a controlled strain rate.

A. Shear-temperature superposition

The nonlinear viscoelastic responses of the three CPCl-Sal solutions have been systematically measured each 5 °C in the range of interest ($T=20$–50 °C). Figure 3(a) displays the long-time shear stress $\sigma(\dot{\gamma})$ as a function of the imposed shear rate for the 12% solution in a semilogarithmic plot. As already mentioned in I, a similar behavior is obtained at all temperatures: The stress increases first linearily in the Newtonian regime and then, at the transition rate $\dot{\gamma}_{I\text{-}N}$ it levels off at the value $\sigma_{I\text{-}N}$. Note that above $\dot{\gamma}_{I\text{-}N}$ a true plateau is found out and that this plateau is only limited at high gradients by some flow instability [19]. It is of the utmost importance to point out here that the constancy of the stress in the plateau regime has been checked very carefully. Different rheological histories were applied to the solutions, e.g., using start-up experiments in which a steady rate is imposed upon a sample initially at rest, or using preshearing either in the Newtonian or in the plateau regimes (see Sec. VII). In all the cases with $\dot{\gamma}>\dot{\gamma}_{I\text{-}N}$, the stress value ends up in the stationary state at $\sigma_{I\text{-}N}$.

The last data point on the flow curve obtained at 30 °C illustrates the effect of an unstable flow on these viscoelastic solutions. The stress drops abruptly and it has been checked that such a drop is associated with the instability described by Larson [19] as the viscoelastic meniscus distortion typical for cone-and-plate device.

As T is increased from 20 to 45 °C, both $\sigma_{I\text{-}N}$ and $\dot{\gamma}_{I\text{-}N}$ are shifted to larger values. However, when passing to the reduced units, σ/G_0 and $\dot{\gamma}\tau_R$, all data points are now superimposed onto a unique flow curve up to the plateau. This is clearly seen in Fig. 3(b) for which the same set of data as those of Fig. 4(a) had been considered. This remarkable superposition was already pointed out in I using different surfactant concentrations but with a unique temperature of measurements ($T=25$ °C).

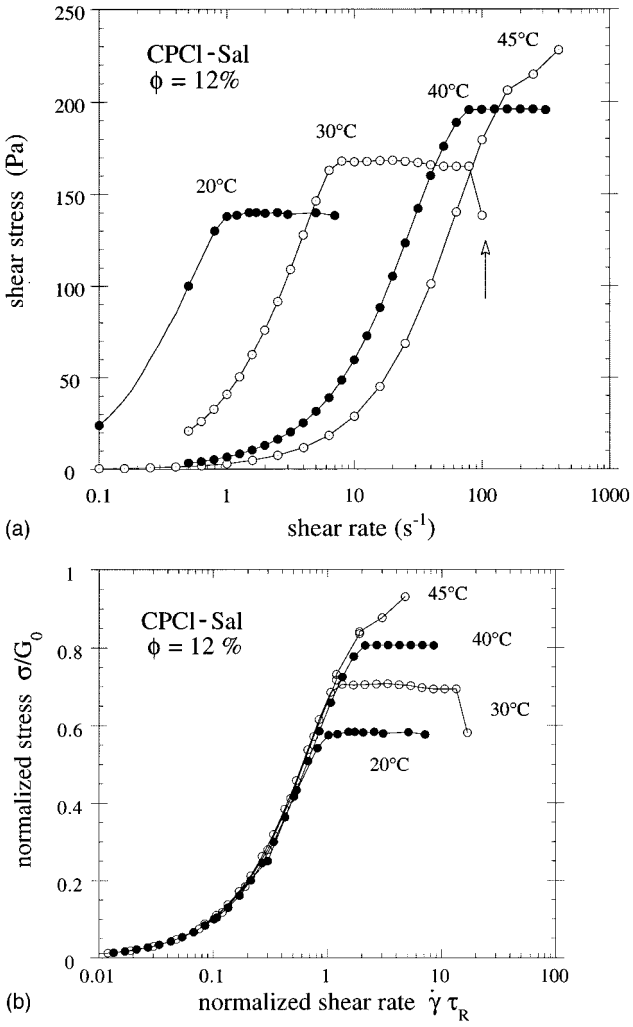

FIG. 3. (a) Shear rate dependencies of the shear stress $\sigma(\dot{\gamma})$ measured for the CPCl-Sal system at $\phi=12\%$ at temperatures varying between 20 °C and 45 °C. All data points of these flow curves were obtained in the stationary limit. The arrow indicating a drop in the stress data at $T=30$ °C refers to a flow instability typical for cone-and-plate devices [19]. (b) Same results as in (a), but using the rescaled units, σ/G_0 and $\dot{\gamma}\tau_R$. Note that at low $\dot{\gamma}\tau_R$, the data points are well superimposed.

B. Shear-concentration-temperature superposition

Up to now, a major drawback has emerged from the nonlinear rheology of the 12% solution displayed in Fig. 3. Changing the temperature is not sufficient to explore a broad range in $\sigma_{I\text{-}N}/G_0$ [at most 30% from Fig. 3(b)] or of different types of flow behavior. This is essentially due to the noticeable variation of the transition rate $\dot{\gamma}_{I\text{-}N}$ with temperature. A way to circumvent this drawback is to show that there is another superposition principle valid for the CPCl-Sal wormlike micelles, namely, the concentration-temperature-shear superpositions. We consider now the two systems at $\phi_1=6\%$ and $\phi_2=8\%$ at the respective temperatures $T_1=20$ °C and $T_2=30$ °C. The viscoelastic Maxwell constants of these two systems are clearly different. They have different linear vis-

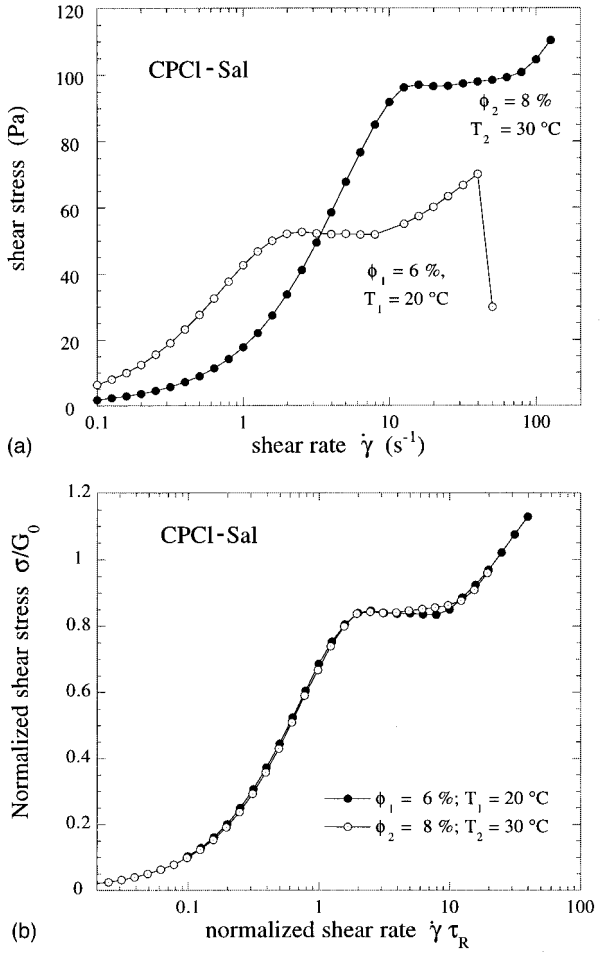

FIG. 4. (a) Shear rate dependencies of the shear stress $\sigma(\dot{\gamma})$ measured for two CPCl-Sal systems (ϕ=6% and ϕ=8%) at two different temperatures, T=20 °C and T=30 °C, respectively. The linear and nonlinear viscoelastic constants related to each solution are listed in Table II. As in Fig. 3(a), the drop in the stress data at ϕ=6% and T=20 °C can be ascribed to some flow instability. (b) Same experimental results as in (a) but using the rescaled units, σ/G_0 and $\dot{\gamma}\tau_R$. Note that now the data points are superimposed for all $\dot{\gamma}\tau_R$ between 10^{-2} up to 50.

coelastic parameters G_0 and τ_R, and when subjected to steady shearing they obey apparently different flow curves [Fig. 4(a)]. The list of their linear and nonlinear characteristics is given in Table II. However, when rescaled in reduced units σ/G_0 and $\dot{\gamma}\tau_R$, Fig. 4(a) demonstrates that they are fully superimposed. The plateau regime occurs here at the same normalized gradient and its height is identical within the experimental accuracy (see Table II for details). This second superposition principle between T and ϕ data is the prerequisite for a master dynamic phase diagram of the CPCl-Sal wormlike micelles in terms of the reduced variables $(\sigma^*, \dot{\gamma}^*, T)$, where $\sigma^* = \sigma/G_0$ and $\dot{\gamma}^* = \dot{\gamma}\tau_R$.

V. MASTER "DYNAMIC PHASE DIAGRAM": REDUCED VARIABLES

We are now in position to derive a generalized flow diagram summing up the behavior under shear at all concentrations and temperatures. For this purpose we first need to develop a systematic (T,ϕ)-correspondence principle inspired from the results of Figs. 3 and 4. For the three micellar solutions investigated in the present work (and in agreement with I), an empirical relationship seems to hold. As temperature is increased (ϕ being fixed), the crossover between the Newtonian and plateau regimes becomes more rounded. With further increase, the $\sigma(\dot{\gamma})$ plateau is replaced by a flat inflexion point. Let us define T_c the critical temperature at which the flat point is observed. At $T=T_c$, we have

$$\sigma_{I\text{-}N}/G_0 = 0.9 \quad \text{and} \quad \dot{\gamma}_{I\text{-}N}\tau_R = 3 \pm 0.5. \tag{3}$$

This temperature T_c obviously depends on the surfactant concentration. Equation (3) is verified for the three solutions (ϕ=6%, 8%, and 12%) studied here at T_c=28, 37, and 48 °C, respectively. The (T,ϕ)-correspondence principle can then be deduced from the data displayed in Fig. 5. Here we have plotted using a semilogarithmic representation the normalized zero-shear viscosity $\eta_0(T)/\eta_0(T_c)$ as a function of the inverse relative temperature $1/T\text{-}1/T_c$ for each concentration, ϕ=6%, 8%, and 12%. All data points align along the same straight line, given by $\eta_0(T)/\eta_0(T_c) = \exp(E_A/k_BT)$ with an Arrhenius energy $E_A = 55k_BT$ (T is taken as the room temperature). Figure 5 can be viewed as follows: it represents the temperature variation of the zero-shear viscosity for a CPCl-Sal micellar solution at a fixed concentration ϕ and for which we would be able to measure the linear and nonlinear viscoelastic responses over a temperature range extending from ~20 °C above T_c to ~30 °C below. As mentioned already, this feature is essentially aimed to overcome the huge variation of $\tau_R(T)$ for a single system.

Figure 6 synthesizes the whole set of normalized flow curves σ^* versus $\dot{\gamma}^*$ obtained on the three different samples, and now expressed in terms of a unique control parameter,

TABLE II. List of the linear and nonlinear viscoelastic quantities as received from measurements on two CPCl-Sal micellar systems at two different temperatures [see also Fig. 4]. Note that despite different linear constants G_0, τ_R, and η_0, the shear stress levels off at the same plateau values $\sigma_{I\text{-}N}/G_0$ and at the same rates $\dot{\gamma}_{I\text{-}N}\tau_R$.

	G_0 (Pa)	τ_R (s)	η_0 (Pa s)	$\sigma_{I\text{-}N}$ (Pa)	$\dot{\gamma}_{I\text{-}N}$ (s^{-1})	$\sigma_{I\text{-}N}/G_0$	$\dot{\gamma}_{I\text{-}N}\tau_R$
ϕ=6%, T=20 °C	62	0.99	62	52	2	0.84	1.98
ϕ=8%, T=30 °C	115	0.16	18	96	12.5	0.83	1.96

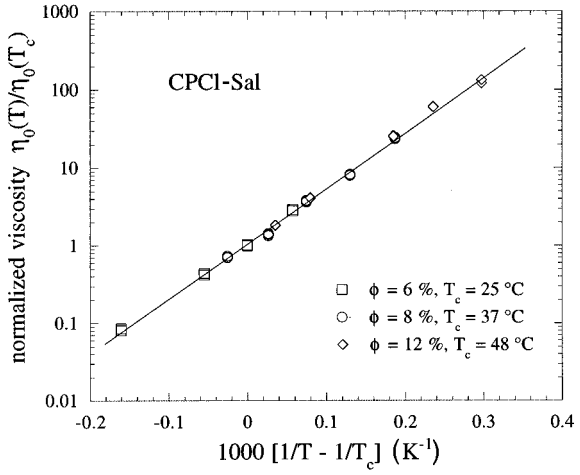

FIG. 5. Using a semilogarithmic representation, the normalized zero-shear viscosity $\eta_0(T)/\eta_0(T_c)$ is plotted as a function of the inverse relative temperature $1/T-1/T_c$ for each concentration, ϕ=6%, 8%, and 12%. T_c is defined for each concentration as the critical temperature (see text). The straight line describes an Arrhenius behavior of activation energy $E_A=55k_BT$. This figure is the basis of the temperature-concentration correspondence principle that was developed here for the CPCl-Sal wormlike micelles.

the temperature, or more precisely the relative temperature with respect to T_c, $T^*=T-T_c$. Values of T^* are shown in Fig. 6 for each selected set of $\sigma^*(\dot\gamma^*)$ data. Below $\dot\gamma\tau_R=1$, all data points in Fig. 6 are superimposed, as expected for the linear Newtonian regime ($\sigma^*=\dot\gamma^*$). The onset of the plateau at $T^*=-28$ °C takes place abruptly and a true discontinuity of slope occurs in the $\sigma^*(\dot\gamma^*)$ behavior. We again point out that the stress plateau at $\sigma^*=\sigma_{I\text{-}N}/G_0$ is robust and that, as far as the stationary state of shearing was concerned, no hysteresis effect could ever be detected using different mechanical histories. As temperature increases toward T_c, the transition is much smoother and the stress levels off without discontinuity. Above T_c no plateau can be detected, the stress increases monotonically, exhibiting an inflection point. Figure 6 illustrates the dynamical phase diagram of micellar solutions subjected to shear in the set of variables, σ^*, $\dot\gamma^*$, and T^*. It resembles strongly that of I, for which the surfactant concentration ϕ was used as control parameter. Note finally that for slightly negative T^* values, the plateau regime is followed by an increase in the stress for reduced shear rates $\dot\gamma^*\sim 20$.

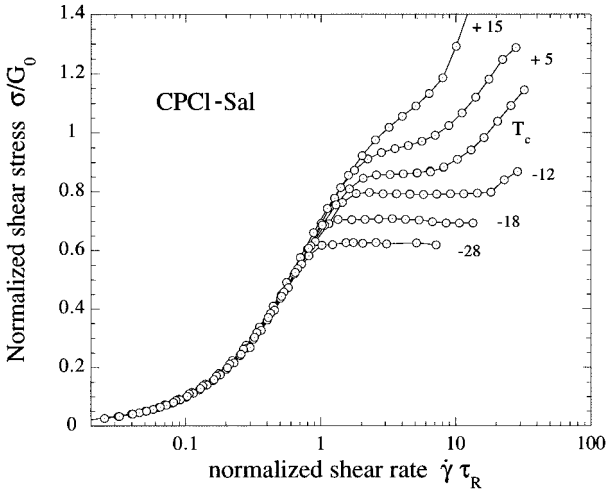

FIG. 6. Master dynamic phase diagram of the CPCl-Sal system. The normalized stress $\sigma^*=\sigma/G_0$ versus $\dot\gamma^*=\dot\gamma\tau_R$ was obtained on three different samples at ϕ=6%, 8%, and 12% and at different temperatures (T=20 °C–50 °C). This phase diagram was derived using the invariance property of the flow curves with respect to temperature and concentration changes. For sake of clarity, only equally spaced curves are shown. They are all identified with respect to the critical temperature T_c, as defined in the text, in terms of the reduced temperature $T^*=T-T_c$ (=−28;+15).

VI. ANALYSIS AND DISCUSSION

The so-called master dynamic phase diagram displayed in Fig. 6 represents one major finding of this paper. It demonstrates first that temperature can also be used as a control parameter to carefully track the smooth evolution between the different flow regimes encountered in the CPCl-Sal wormlike micelles, namely, the regime of a true plateau with a discontinuity in slope in the $\sigma^*(\dot\gamma^*)$ behavior, the critical regime without an abrupt crossover, then the regime characterized by a monotonic increase of the stress. Second, the precise knowledge of the linear viscoelasticity enables us to work with the reduced rheological quantities $\sigma^*=\sigma/G_0$ and $\dot\gamma^*=\dot\gamma\tau_R$. We here take advantage of the fact that the CPCl-Sal system can be considered as an almost perfect Maxwellian fluid in this temperature and concentration range. In the following section, we briefly bring to mind some results and interpretations of our previous works [7,10] that lead us to interpret the overall nonlinear response in terms of isotropic-to-nematic transition induced by shear.

In our previous papers [7,10], we claimed that the σ^* plateau could be interpreted as the coexistence line of two different thermodynamical phases present within the shearing cell. These two phases, isotropic and nematic, were assumed to coexist all along the stress plateau and under these conditions, the shear rate should act only on the relative proportions of each phase. The arguments developed in I for such a conclusion were based on (i) the formal analogy of the transient shear stress behaviors obtained in start-up experiments on both CPCl-hexanol-brine (at ϕ=32% [6]) and CPCl-Sal systems; (ii) a strong experimental indication for the CPCl-hexanol-brine solution of two coexisting phases of different order parameters [6], indicating a biphasic isotropic-nematic stable state. This latter result was revealed using small-angle neutron scattering under shear in the same $\dot\gamma$ regime.

For both surfactants, transient stresses were recorded in start-up experiments at shear rates above the discontinuity of slope, i.e., for $\dot\gamma>\dot\gamma_{I\text{-}N}$, and were shown to be analytically similar. The time evolution of the shear stress could be fitted according to a stretched exponential of the form

$$\sigma(t,\dot\gamma)=\sigma(t\to\infty,\dot\gamma)+\Delta\sigma_0\exp\left(-\frac{t^2}{\tau_N^2(\dot\gamma)}\right), \qquad (4)$$

where $\sigma(t\to\infty,\dot\gamma)=\sigma_{I\text{-}N}$ denotes the long-time stationary values of the stress, $\Delta\sigma_0$ the amplitude of the overshoot after inception of the shearing, and $\tau_N(\dot\gamma)$ a typical time com-

prised between 10 and 300 s, depending on the shear rate applied [$\tau_N(\dot\gamma)$ decreases rapidly with increasing $\dot\gamma$]. A preliminary report of the trend quoted by Eq. (4) was published in Refs. [7, 10]. Actually, $\tau_N(\dot\gamma)$ was related in I to a typical time featuring both the nucleation and the growth processes of the oriented phase in coexistence with the remaining isotropic one. The interpretation in terms of nucleation and one-dimensional growth dynamics (domain of metastability) was considered as a strong indication of a first-order character of the *I-N* transition. Equation (4) indicates moreover that the stress versus time is a decreasing function (overshoot situation). This overshoot is in good agreement with the expectation that the nematic state induced by shear has a much lower viscosity than the coexisting isotropic one. It was finally concluded that the *I-N* transition in wormlike micelles was associated with an organization of the solution into macroscopic layers of different order parameters and velocity gradients.

The present data reported in Sec. V are in full agreement with I and [10]. But in addition, we here show that the flow behavior—in reduced units—can be monitored by changing either concentration or temperature. The correspondence between concentration and temperature is given by the evolution of the critical temperature versus ϕ: $T_c(\phi)$. Then the entire set of flow behaviors can be drawn as functions of σ^*, $\dot\gamma^*$, and $T^*=T-T_c(\phi)$. Interestingly, the critical flow conditions are $\sigma^*=0.9$ and $\dot\gamma^*=3$ [see Eq. (3)]. According to us, these remarkable invariances have a deep physical meaning that we think is contained in the evolution $T_c(\phi)$. But a complete rheological characterization of this variation is indeed difficult. Above 50 °C, evaporation makes measurements unreliable whereas below 20 °C the system precipitates. So the temperature range accessible is far too narrow.

A. Nonequilibrium phase diagram

As mentioned in the introductory part, a strong motivation to reexamine the nonlinear rheology of the CPCl-Sal wormlike micelles as a function of temperature was related to some recent theoretical works due to See, Doi, and Larson [16] and Olmsted and Goldbart [17]. These authors have solved the problem of shear-induced *I-N* phase transition for rigid rodlike polymers. Although isotropic solutions of rigid rodlike polymers (low molecular weight) cannot be assimilated to the viscoelastic system made of long flexible surfactant aggregates, the qualitative analogies between their conclusions and those drawn in I deserve some extra comment. Using basically different approaches, these two groups converge to the same findings. When subjected to a flow field, and in particular to a shearing field, rodlike molecules in the isotropic state undergo a phase transition toward a nematic state. More interesting for us is the nonequilibrium phase diagram predicted by Olmsted and Goldbart using a free-energy approach including explicit coupling between the nematic order parameter and the fluid velocity fields [17]. This phase diagram is expressed in terms of reduced shear stress and temperature, noted s^* and τ, respectively (notations are those of Ref. [17], see Fig. 9). For temperatures comprised between $\tau_{I\text{-}N}$ (the isotropic-nematic transition temperature in absence of flow) and the critical value $\tau^*>\tau_{I\text{-}N}$, with increasing stress, there exists a two-state region with two locally stable states, isotropic and nematic,

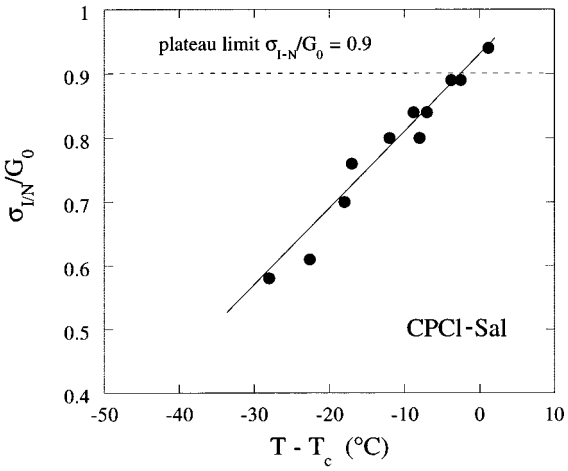

FIG. 7. First nonequilibrium phase diagram for the CPCl-Sal wormlike micelles. Here, the reduced stress at the plateau $\sigma_{I\text{-}N}/G_0$ determined from the nonlinear viscoelastic responses is shown against T^*, the temperature relative to T_c. The data points obtained at different temperatures and concentrations are found to roughly align on a straight line that ends up at the critical point $\sigma^*=0.9$; $T=T_c$.

characterized by differing order parameters and velocity gradients. In others words, the solution would exhibit a locally stable inhomogeneous flow. For temperatures larger than τ^*, no transition occurs.

With the set of data obtained in the above sections for CPCl-Sal wormlike micelles, we have been able to construct a nonequilibrium phase diagram, analogous to that proposed by Olmsted and Golbart [17]. It is shown in Fig. 7, where the reduced stress at the plateau $\sigma_{I\text{-}N}/G_0$ is plotted against T^*, the temperature relative to T_c. All the data points deduced from the height of the σ^* plateau roughly align on a straight line (also indicated in Fig. 7) and the coordinates of the critical point are $s^*=0.9$ and $T=T_c$. If one accepts the picture of the *I-N* transition terminated with a critical behavior at T_c, this straight line separates two domains of different symmetries (orientational order).

Likewise, Fig. 8 has been constructed using the reduced shear rates $\dot\gamma_{I\text{-}N}\tau_R$ plotted against the relative temperature $T-T_c$. The full circles are deduced from the first crossover observed between the Newtonian and plateau regimes whereas the empty circles indicate the onset of further increase of the shear stress σ^* (see Fig. 6). At a fixed temperature below T_c, full and empty circles thus delimitate the range of the stress plateau. As will be shown below, the continuous line is interpreted as the boundary between two different states of shearing. At low $\dot\gamma^*$ or at temperature larger than T_c, the flow is considered to be homogeneous. At rates $\dot\gamma^*>\dot\gamma_{I\text{-}N}\tau_R$, the solution is organized into macroscopic layers subjected to different shear gradients, and the flow is inhomogeneous.

The qualitative resemblance between predictions (Fig. 9 in [17]) and experimental results of Fig. 7 is spectacular. This agreement should not be overestimated, however, at least for two reasons: (i) Ref. [16] deals with rigid rodlike polymer solutions while Ref. [17] is suited for low molecular weight molecules of thermotropic mesogens: wormlike micelles are very long and very flexible polymerlike chains. (ii)

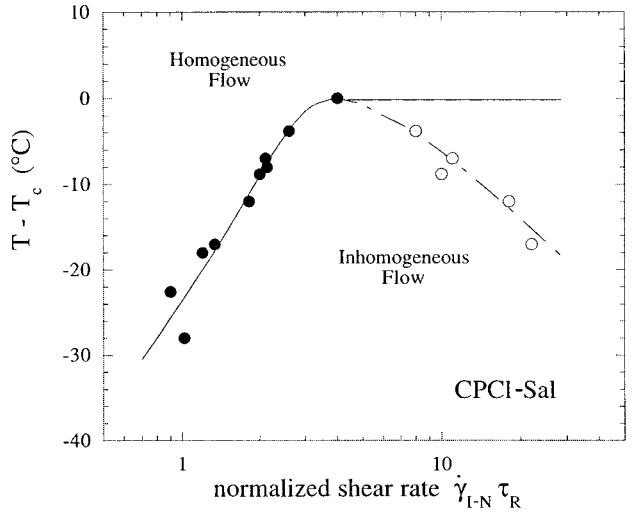

FIG. 8. Second nonequilibrium phase diagram for the CPCl-Sal wormlike micelles. Here, the reduced temperature $T-T_c$ is displayed as a function of the rescaled shear rate $\dot{\gamma}_{I\text{-}N}\tau_R$. The full circles are determined from the first crossover observed between the Newtonian and plateau regimes whereas the empty circles indicate the onset of further increase of the shear stress σ^*, occurring at $\dot{\gamma}^*>10$ (see Fig. 6). The continuous line indicates the boundary between homogeneous and inhomogeneous states of shearing.

In Fig. 7, we have assumed *a priori* that the flow curve $\sigma^*(\dot{\gamma}^*)$ displaying a flat point refers to a critical behavior, indicating either a critical temperature or concentration. This assumption has been founded on rheological measurements only, but was never proved explicitly from, i.e., scattering experiments.

B. Flow birefringence

Despite numerous attempts to elucidate the transition in CPCl-Sal wormlike micelles using small-angle neutron scattering (SANS) under shear, we never arrive at an unambiguous description, as the one obtained for the CPCl-hexanol-brine system in [6] and described above. A clear identification of two phases differing in orientational order was not straightforward. Thus, in order to examine the state of shearing at the stress plateau, flow birefringence (FB) experiments were undertaken with a rheo-optical device working under basically different conditions, as compared to the standard Couette cell needed for neutrons. For the flow birefringence, measurements were carried out using a 1.5 mm gap Couette cell as shearing device. However, here the polarized white light is sent in the direction of vorticity, that is, along the cell height (30 mm) perpendicular to the plane defined by the fluid velocity and to the shear gradient. More details on the FB experiment can be found in Ref. [22]. We do not aim to present in this preliminary report results on the shear rate dependencies of the extinction angle χ and birefringence Δn. Instead, we visualized the state of the sheared sample between crossed polarizers. The pair of crossed polarizers is set in a position that lets one arm of the cross of isocline appear in the field of observation. The sample placed under scrutiny was the CPCl-Sal solution at $\phi=12\%$ and $T=28$ °C. According to the results of Fig. 3(a) the transition shear rate is estimated at $\dot{\gamma}_{I\text{-}N}=5\pm1\ \mathrm{s}^{-1}$ for a stress leveling off at $\sigma_{I\text{-}N}=160\pm2$ Pa.

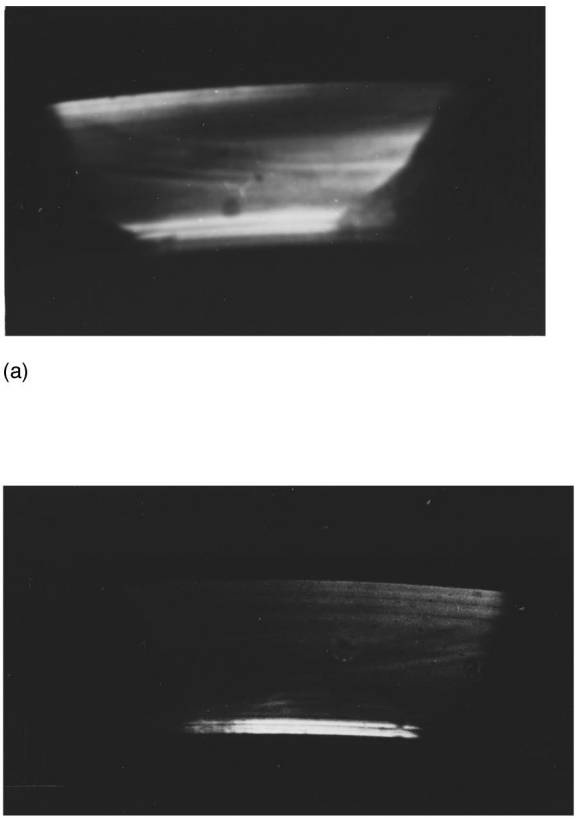

FIG. 9. Photographs of the 1.5-mm gap of a Couette shearing cell containing a CPCl-Sal solution at $\phi=12\%$ and $T=28$ °C. In this flow birefringence experiment, the polarized white light is sent in the direction of vorticity and the pairs of crossed polarizers is set in a position that lets one arm of the cross of isocline appear in the field of observation. For this experiment, we remember that the transition shear rate is estimated at $\dot{\gamma}_{I\text{-}N}=5\pm1\ \mathrm{s}^{-1}$ for a stress leveling off at $\sigma_{I\text{-}N}=160\pm2$ Pa. The two photographs correspond to the following shear histories: (a) under shear at $\dot{\gamma}=10\ \mathrm{s}^{-1}$, i.e., in the plateau regime; (b) at rest, a few seconds after cessation of the shear at $\dot{\gamma}=10\ \mathrm{s}^{-1}$.

Figure 9(a) shows a photograph of the 1.5-mm-gap under steady shear at $\dot{\gamma}=10\ \mathrm{s}^{-1}$, i.e., in the plateau region. The sheared solution in Fig. 9(a) exhibits strong coloration that progressively changes when going from the outer to the inner walls of the Couette. The colors reflect the large birefringence of the CPCl-Sal solution. At low shear rate, say $1\ \mathrm{s}^{-1}$, Δn approaches 10^{-5}, a value that agrees with the value of the birefringence in similar micellar solutions, e.g., CTAB-NaSal [23]. A closer inspection reveals, however, two distinctive regions. One close to the inner cylinder is made of a succession of very thin and unicolor (striated) bands. In the rest of the gap, bands are much broader and the colorations vary more progressively. From the photograph taken at $10\ \mathrm{s}^{-1}$, one can roughly estimate that the striated layer occupies $\frac{1}{10}$ of the whole gap, but its spatial extension is not easy to determine.

Once the stationary regime of shearing has been reached at $10\ \mathrm{s}^{-1}$, the rotation is stopped abruptly, and a photograph is shot a few seconds after cessation of the shear, resulting in Fig. 9(b). Figure 9(b) exhibits now clearly two separate re-

gions of very different birefringence. This photograph resembles strongly the ones reported by Cappelaere and coworkers on salt-free concentrated CTAB solutions under shear [8,9]. Here, the spatially dominating layer (close to the outer cylinder) relaxes very rapidly and appears to be dark between the polarizers, indicating an isotropic refractive index tensor. On the contrary, the striated layer composed by the thin banding evoked above still remains very bright. Its complete relaxation actually requires several seconds. From the relaxation of the FB after cessation of shear, we conclude that the orientation of the wormlike micelles and thus the optical anisotropy tensors in both inner (striated) and outer layers of Fig. 9(a) are different under shear. This demonstrates that in the plateau regime the flow is inhomogeneous. In the striated band, the wormlike micelles are strongly oriented with respect to the flow. This region supports a much larger shear gradient than the outer layer and its relative proportion is determined to accommodate the imposed macroscopic velocity gradient $\dot{\gamma}$. Note, finally, two qualitative observations in agreement with the transition from homogeneous to inhomogeneous flow: the striated layer only shows up as the solution was sheared above $\dot{\gamma}_{I\text{-}N}$ and its relative proportion increases with increasing shear rates.

Extension of these preliminary data are under progress, concerning, in particular, the measurements of the extinction angle χ and birefringence Δn, as well as the amount of oriented phase as a function of $\dot{\gamma}$. The assignment of the oriented striated layer to a nematic state induced by shearing would be available by closely comparing the data received from flow birefringence and small-angle neutron scattering.

VII. CONCLUSIONS

The major findings of this paper are the master dynamic phase diagram of the CPCl-Sal wormlike micelles using the temperature as a controlled parameter, and the experimental evidence that these micelles flow inhomogeneously. By inhomogeneous flow, we mean that the solution is organized under shear into macroscopic layers subjected to different shear gradients.

The dynamic phase diagram has been derived using superposition principles evidenced on the flow behavior obtained as a function of temperature (T=20 °C–50 °C) and concentration (ϕ=6–12 %). The generality of this phase diagram arises from the fact that it uses the reduced rheological quantities σ/G_0 and $\dot{\gamma}\tau_R$ instead of σ and $\dot{\gamma}$. It should be emphasized that the flow phase diagram of Fig. 6 can be obtained similarly by changing either the micellar concentration ϕ or the temperature T. Having introduced for each concentration ϕ the critical temperature $T_c(\phi)$, the complete set of flow behaviors is then totally specified by the three reduced variables, σ^*, $\dot{\gamma}^*$, and T^*. Flow birefringence reveal interesting but very complex features for the CPCl-Sal solutions. It was therefore out of the scope of the present paper to go beyond a brief description. Figure 9 demonstrates in this respect that the plateau regime occurring with a true discontinuity of slope in the $\sigma^*(\dot{\gamma}^*)$ data is actually connected with an inhomogeneous flow of the solution. The stress plateau obtained in these controlled rate measurements does correspond to the coexistence line of two stable phases differing in viscosity, orientation, and order parameters.

In conclusion, it is worthwhile mentioning that very recently, similar nonhomogeneous flows have been observed too in semidilute surfactant solutions by means of NMR imaging methods [24]. This latter phenomenon was ascribed to some ''spurt effect'' adapted for wormlike micelles.

ACKNOWLEDGMENTS

The authors would like to acknowledge Emmanuel Cappealere, Jim Harden, François Molino, Peter Olmsted, and Lynn Walker for fruitful discussions.

[1] H. Rehage and H. Hoffmann, Mol. Phys. **74**, 933 (1991), and references therein.
[2] M. E. Cates and S. J. Candau, J. Phys. Condens. Matter **2**, 6869 (1990).
[3] M. E. Cates, Macromolecules **20**, 2289 (1987).
[4] R. Granek and M. E. Cates, J. Chem. Phys. **96**, 4758 (1992).
[5] V. Schmitt, F. Lequeux, A. Pousse, and D. Roux, Langmuir **10**, 955 (1994); V. Schmitt, Thèse de Doctorat, Université de Strasbourg, 1994 (unpublished).
[6] J.-F. Berret, D. C. Roux, G. Porte, and P. Lindner, Europhys. Lett. **25**, 521 (1994); D. C. Roux, Thèse de Doctorat, Université de Montepellier, 1995 (unpublished).
[7] J.-F. Berret, D. C. Roux, and G. Porte, J. Phys. **4**, 1261 (1994).
[8] E. Cappelaere, R. Cressely, and J.-P. Decruppe, Colloids Surf. **104**, 353 (1995); E. Cappelaere, Thèse de Doctorat, Université de Metz, 1995 (unpublished).
[9] J.-P. Decruppe, R. Cressely, R. Makhloufi, and E. Cappelaere, Colloid Polym. Sci. **273**, 346 (1995).
[10] J.-F. Berret, D. C. Roux, and G. Porte, in *Proceedings of the IVth European Conference on Rheology, Seville, 1994,* edited by C. Gallegos (Steinkopf, Darmstadt, 1994), p. 582.
[11] E. Cappelaere, J.-F. Berret, J.-P. Decruppe, R. Cressely, and P. Lindner (unpublished).
[12] V. Schmitt, C. Marques, and F. Lequeux, Phys. Rev. E **52**, 4009 (1995).
[13] J. F. Berret, J. Appell, and G. Porte, Langmuir **9**, 2851 (1993).
[14] N. A. Spenley, M. E. Cates, and T. C. B. MacLeish, Phys. Rev. Lett. **71**, 939 (1993).
[15] N. A. Spenley, X. F. Yunan, and M. E. Cates, J. Phys. (France) II **6**, 551 (1996).
[16] H. See, M. Doi, and R. Larson, J. Chem. Phys. **92**, 792 (1990).
[17] P. Olmsted and P. Goldbart, Phys. Rev. A **46**, 4966 (1992).
[18] H. Rehage and H. Hoffmann, J. Phys. Chem. **92**, 4712 (1988).
[19] R. G. Larson, Rheol. Acta **31**, 497 (1992).
[20] Lynn Walker (private communication).
[21] F. Kern, R. Zana, and S. J. Candau, Langmuir **7**, 1344 (1991).
[22] J.-P. Decruppe, R. Hocquart, T. Wydro, and R. Cressely, J. Phys. (France) **50**, 3371 (1989).
[23] T. Shikata, S. J. Dahman, and D. S. Pearson, Langmuir **10**, 3470 (1994).
[24] P. T. Callaghan, M. E. Cates, C. J. Rofe, and J. B. A. F. Smeulders, J. Phys. (France) **6**, 375 (1996).